Carbohydrate Fluxes into Alginate Biosynthesis in *Azotobacter vinelandii* NCIB 8789: NMR Investigations of the Triose Pools[†]

John M. Beale, Jr.,* and Jennifer L. Foster

Division of Medicinal and Natural Products Chemistry, College of Pharmacy, The University of Texas at Austin, Austin, Texas 78712-1074

Received August 15, 1995; Revised Manuscript Received October 26, 1995[⊗]

ABSTRACT: The metabolite flux of carbohydrates through primary catabolism and into hexose resynthesis has been investigated for alginic acid biosynthesis in *Azotobacter vinelandii*. To do these studies, we fed the microorganism a variety of ^{13}C-labeled glucose precursors, including [U-$^{13}C_6$]glucose. The incorporations of the precursors were determined by 1D ^{13}C-NMR, 2D ^{13}C-DQF-COSY, and inverse triple-quantum correlation experiments. The results clearly show that the entire catabolism of hexose is through the Entner−Doudoroff (E−D) pathway and that the triose pools are in equilibrium. Reentry into gluconeogenesis prior to alginate synthesis occurs totally from the glyceraldehyde 3-phosphate generated by the E−D pathway. The obligatory intermediacy of triose intermediates in alginate biosynthesis was proved. The experiments and results presented in this paper constitute a new method for distinguishing the E−D pathway from glycolysis in bacteria.

Alginate (Figure 1) is a nonbranched 1→4-linked polymer of β-D-mannuronate (M or ManA)[1] and its C-5 epimer, α-L-guluronate (G or GulA) (Steginsky & Beale, 1992; Gacesa, 1988; Larsen & Haug, 1971a,b). The structure, chemistry, and viscosity properties of alginate solutions have been extensively reviewed (Gacesa, 1988; Beale & Steginsky, 1990). The applicability of the viscosity properties to food, drug, and cosmetic preparations accounts for the commercial importance of alginate. Alginate is the main cellular constituent of brown algae such as *Phaeophytaceae*, *Macrocystis*, and *Fucus*, and these are the chief commercial sources of the polymer. Only two bacterial genera, *Azotobacter* and *Pseudomonas*, are known to produce the polysaccharide. Of these, alginate-producing (mucoid) strains of *Pseudomonas aeruginosa* commonly cause intractable pulmonary infections in cystic fibrosis (CF) patients (Russell & Gacesa, 1988). The nature of the morbidity and mortality of these infections has been recently reviewed (Russell & Gacesa, 1988). At present, there is no treatment for infections by mucoid pseudomonads. Knowledge of the key enzymes and intermediates of the biosynthetic pathway of alginate, and the manner in which these differ from similar routes of carbohydrate metabolism in humans, may lead to new targets for therapeutic intervention.

The steps of the late-stage biosynthesis of alginate have been studied by several groups (Lin & Hassid, 1966a,b; Larsen & Haug, 1971; Gacesa, 1988; Skjåk-Bræk & Larsen, 1971). There is general agreement that the pathway from fructose to alginate is the same in algae such as *Fucus gardneri* and bacteria like *P. aeruginosa* and *Azotobacter vinelandii*. The general pathway, shown in Figure 2, was deduced through sugar nucleotide characterization and enzyme detection. Chakrabarty and Ohman (Chakrabarty et al., 1990; Darzins & Chakrabarty, 1984; Ohman et al., 1990) have studied the genetics of the pathway extensively, and many nonmucoid constructs have been made. Today, the only mechanistic unknowns involve the terminal steps, the acetylation/deacetylation, polymerization, and C5′ epimerization. Some of Chakrabarty's work has focused on the tendency for mucoid (alginate-producing) *P. aeruginosa* to undergo a spontaneous phenotypic shift to a nonmucoid type. This tendency complicates studies on alginate biosynthesis, so we chose *A. vinelandii* as the prototype alginate producer for our studies.

The "early" steps of the biosynthetic pathway (those leading from hexose substrate to fructose) are of interest to us because they represent the chemistry at the interface of primary and secondary metabolism. Most studies of natural product biosynthesis involve developing a set of logical precursors, preparing or buying them in labeled form, and tracking them through the secondary metabolic pathway through feeding experiments (Floss & Beale, 1989). Working backward from the distribution of the label in the product, the nature of the pathway should be revealed. When the natural product is a carbohydrate produced by a bacterium *growing on* a carbohydrate, a complex set of channeling possibilities results. In the case of a hexose, the growth substrate must be catabolized, routed through primary metabolic pools (which may be in equilibrium with other pools through common intermediates), resynthesized into "new" hexose, and assembled into the final product. Six reports of studies on the channeling of intermediates of primary metabolism into the terminal sequence of polyuronate biosynthesis have appeared (Carlson & Matthews, 1966; Pindar & Bucke, 1975; Lynn & Sokatch, 1984; Wingender et al., 1985; Anderson et al., 1987; Banerjee et al., 1983). These studies were generally consistent and showed three obvious results: (1) radiolabel from [6-^{14}C]-

[†] This work was supported by National Institutes of Health Grant GM47642 (to J.M.B.).

* Author to whom correspondence should be addressed.

[⊗] Abstract published in *Advance ACS Abstracts,* February 1, 1996.

[1] Abbreviations: M or ManA, mannuronic acid; G or GulA, guluronic acid; E−D, Entner−Doudoroff pathway; E−M−P, Embden−Meyerhof−Parnas pathway; TCA, tricarboxylic acid cycle; TQ, triple quantum; DQ, double quantum; TPPI, time-proportional phase incrementation; COSY, correlation spectroscopy; NMR, nuclear magnetic resonance; NOE, nuclear Overhauser effect.

0006-2960/96/0435-4492$12.00/0

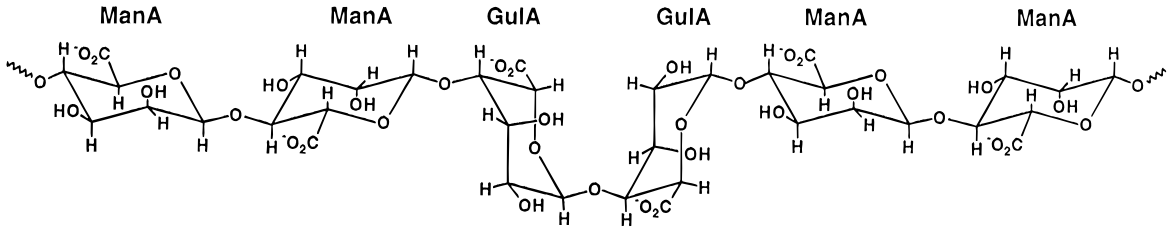

FIGURE 1: Chemical structure of a representative segment of alginic acid.

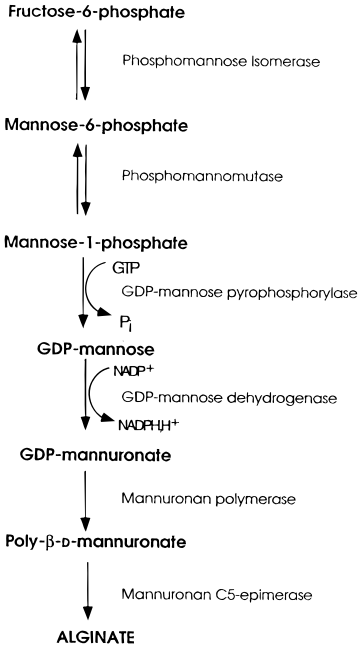

FIGURE 2: Proposed "terminal sequence" of the biosynthetic pathway to alginate.

glucose is incorporated 10−160 times greater than label from [1-^{14}C]glucose; (2) the specific radioactivity of the product is greater than that of the precursor fed; (3) label from [^{14}C]-fructose was incorporated equally well from the 1- and 6-positions. Additionally, Lynn and Sokatch (1984) showed that label from [2-^{14}C]glucose was incorporated at approximately twice the rate as that from the 1-labeled precursor. These results suggest two possibilities: (1) there is an obligatory involvement of trioses in the pathway, and at some time during biosynthesis two fluxes of labeled intermediates enter from more than one pool and are combined to form a labeled metabolite with a specific incorporation higher than that of the precursor; and (2) the labeling patterns are consistent with catabolism of hexose by the Entner−Doudoroff (E−D) pathway, which is a low-energy-yielding pathway common to many Gram-negative bacteria.

The previously mentioned studied were published before sensitive stable isotope/NMR methods became commonplace, and radioisotopically labeled precursors were used as metabolic tracers. With the exception of Carlson's work, the products were not chemically degraded to locate and quantitate the label unequivocally. Carlson and co-workers made no attempt to prove that the polymer from these experiments was in fact alginate. The set of reports is consistent in its implication of the E−D pathway in *P. aeruginosa* and *A. vinelandii*, but a more detailed picture is needed for reasons that will be given below.

Normally, predictions of the biosynthesis of a secondary metabolite are based on fundamental chemical and biochemical knowledge. We have previously shown (Degwert et al., 1987; Rohr et al., 1989) that predictions of isotope incorporation on carbohydrate biosynthesis based on fundamental biochemical knowledge may be in error. As we reported for the α-glucosidase inhibitor acarbose and the urdamycin antibiotics (Rohr et al., 1989), the metabolic pools of triose intermediates such as glyceraldehyde 3-phosphate, dihydroxyacetone phosphate, and pyruvate may not be in equilibrium, and labeling patterns can be different from predictions. In both of our studies, isotope sugar labeling patterns were consistent with the E−D and not the Embden−Meyerhof−Parnas (E−M−P) pathway, despite the fact that *Streptomyces* species, being Gram-positive bacteria, are known to utilize the E−M−P pathway for hexose catabolism unless induced by growth on gluconate. Our cultures were not induced in this manner.

More daunting is the possibility that pathway overlap occurs. The pentose phosphate pathway is found throughout the microbial world and is a secondary source of fructose and glyceraldehyde 3-phosphate. The fructose from this pool may contain up to eight different isotopomers from [U-^{13}C]-glucose. Cycling through the tricarboxylic acid pathway or direct incorporation of precursor may occur. The different labeling patterns and percentages of intermediates from overlapping pathways, all of which can feed into the alginate pathway, can render radioisotope studies useless.

In this paper, we report the application of stable isotope feedings coupled with selective NMR methods to the problem of unraveling metabolite channeling from glucose into alginate biosynthesis in *A. vinelandii*. The results clearly show that in *A. vinelandii* the major metabolite flux involves obligatory triose intermediates and that the E−D pathway is the major route of glucose catabolism. There is no detectable direct incorporation of glucose, and the high incorporation rates from C1, C3, and C4 rule out processing past the triose stage by pyruvate decarboxylase. The triose pools feeding alginate biosynthesis are, in this case, in equilibrium. The multiple labeling experiments provided a unique opportunity to observe dilution during biosynthesis and proved that the direction of epimerization proceeds in the same direction as the polymerization of GDP-mannuronic acid.

MATERIALS AND METHODS

Microorganism. We obtained *A. vinelandii* NCIB-8789 from the Microbiology Department Culture Collection at The Ohio State University (accession number OSU-413). Phase-contrast microscopy and comparison with descriptions in Bergey's Manual of Determinative Bacteriology confirmed the identity and purity of the strain. To maintain viability, we transferred the organism to fresh agar medium at 2 week intervals and conducted experiments with 96-h-old inocula. Sealed, screw-capped tubes of agar were used for long-term storage at 4 °C.

General. We obtained organic medium components and buffers from Difco Laboratories or Sigma Chemical Co., and all were of microbiology grade or better. Fisher Scientific Co. supplied inorganic medium components, which were of analytical grade or better. Spectrapor dialysis membranes were purchased from Baxter Scientific Products, Inc. Isotec, Inc., Miamisburg, OH, supplied precursor compounds D-[1-^{13}C]-, D-[2-^{13}C]-, D-[6-^{13}C]-, and D-[U-$^{13}C_6$]glucose. These were at minimum 99 atom % ^{13}C. We confirmed the purity and label position of all precursors by ^{13}C-NMR spectroscopy. Deuterium oxide ampules for NMR were from Aldrich and were 100 atom % ^{2}H. A nanopure four-chamber purifier was used to prepare deionized water (conductance = 18 MΩ/cm) for fermentation media. Sterile syringe filters, 0.22 μm pore size, were purchased from Gelman.

Culture and Fermentation Protocol. Cultures of *A. vinelandii* NCIB-8789 were cultivated for 4 days at 29 °C on agar slants of Larsen's medium B (Larsen, 1971). Larsen's medium B consisted of (amounts per liter) D-glucose, 20 g; K_2HPO_4, 1 g; $MgSO_4 \cdot 7H_2O$, 0.2 g; $FeSO_4 \cdot 7H_2O$, 0.05 g; $CaCl_2$, 0.015 g; $NaMoO_4 \cdot 2H_2O$, 0.005 g; NH_4-OAc, 2.3 g; Bacto agar, 15.0 g; H_2O to make 1 L. The pH of the agar medium was adjusted to 7.0 with 1 N HCl before dissolution of the agar and autoclaving. Glucose was autoclaved separately from the salts and added to make the complete medium after cooling. Alginate production experiments were conducted according to a single-stage fermentation protocol in liquid Larsen's medium B, in 500 mL foam-plugged Erlenmeyer flasks, each containing 100 mL of medium. Each 100 mL of liquid medium was inoculated with the contents of one slant and incubated at 300 rpm and 29 °C in a New Brunswick Scientific Innova gyrotory shaker (1 in. throw). Under these conditions, after a brief lag phase, cell mass increased to a maximum at 24 h. At this time, the onset of polyuronate biosynthesis was detectable by the appearance of 2-propanol-precipitatable material in the medium. The precipitate reacted positively with the modified carbazole reagent (Knutson & Jeanes, 1968), which is a standard for detection of uronic acids. The biosynthetic phase could be followed by measuring the increase in carbazole-reactive product after 24 h. After about 72 h of incubation, the total uronic acid content in the medium reached a plateau, and the fermentation was harvested. Since feeding experiments were conducted with short incubation times, no special precautions were taken to inhibit alginate lyase, an enzyme produced late in the fermentation that depolymerizes alginate.

Isolation of Alginate from A. vinelandii NCIB 8789. Cultures were pooled and made 100 mM in NaCl and 10 mM in Na_2EDTA to break the alginate−calcium complex, facilitating the removal of bacterial cells. Centrifugation of 20000*g* and 4 °C in a Sorvall RC-5 centrifuge for 30 min yielded a clear supernatant which was decanted. The pellet containing the cells was discarded. Alginate was precipitated from the aqueous supernatant by addition of two volumes of cold 2-propanol. The polysaccharide precipitated immediately, and the viscous mass was removed by winding onto a glass rod. The precipitated alginate was then suspended in 100 mL of deionized water, solubilized by adjusting to pH 8.0 with 1 M NaOH, and dialyzed overnight against 50 mM EDTA (pH 8.0) in Spectrapor dialysis membranes (3500 MW cutoff). Each dialysis bag was then placed in a beaker containing 4 L of water, and the EDTA was removed by exhaustive dialysis over 24 h, changing the water every 6 h. Samples were lyophilized (SpeedVac, Savant Instruments), and the alginate was collected as a white fibrous, fluffy material. A typical 1.0 L fermentation yielded about 250 mg of dried, purified alginate.

Feeding Experiments with Stable Isotope-Labeled Precursors. Stable isotope feeding experiments were conducted according to the single stage fermentation protocol previously outlined. After inoculation, the cultures were incubated for 24 h until the onset of alginate biosynthesis. A 75 mg/mL stock solution of each ^{13}C-labeled glucose was prepared in deionized water, and the precursor was added to the cultures by sterile filtration through 0.22 μm Gelman syringe filters. A quantity of 250 mg of labeled glucose was fed to each culture (total 1 g) according to a four-dose procedure in which 25 mg/flask was added at 15 h incubation and 75 mg/flask at 18, 21, and 24 h. No dilution with unlabeled carrier was made. Incubation was continued for an additional 20 h, and the alginate was harvested and purified as described above.

Fractionation of Alginate Samples. Though NMR studies were possible on native alginate, signal interpretation and quantitation were facilitated by partial hydrolysis of the polysaccharide to obtain blocks of residues of dP ≈ 20 (Steginsky & Beale, 1992). At the same time, differential fractionation of the hydrolysate provided separate oligomannuronate and oligoguluronate blocks for study. Solid alginate was wetted with a small amount of glycerol, and the sample was suspended in 0.3 M aqueous HCl [1:10 (w/v)]. The suspension was refluxed for 2 h, then cooled on ice, and centrifuged. The supernatant (fraction 1), contining acid-soluble random ManA/GulA blocks, was discarded, while the pellets were redissolved in water by adjusting to pH 8.0 with 1 M NaOH. Differential precipitation by careful addition of 1 M HCl yielded two precipitates. Fraction 2, which precipitated at pH 2.85, contained oligoguluronic acid, and fraction 3, which precipitated at pH 1.6, contained oligomannuronic acid. Fractions 2 and 3 were redissolved at pH 8.0 and then exhaustively dialyzed against water (M_r 3500 cutoff). This treatment provided clean oligo-ManA and oligo-GulA fractions which were of dP ≈ 20 as determined by ^{1}H-NMR spectroscopy (Steginsky & Beale, 1992). The ratios of the integrals of the internal H1 or H2 signals to the integral of the single reducing end H1 signal were used to determine the dP. Statistical characterization was also accomplished by ^{1}H-NMR spectroscopy. These methods will be discussed below.

NMR Spectroscopy. One- and two-dimensional NMR spectra were acquired on a Bruker AMX-500 instrument operating at a field strength of 11.75 T (500.1 MHz ^{1}H and 125.1 MHz ^{13}C). Either 5 mm diameter dual carbon/proton or 5 mm inverse probes were used. Wilmad no. 528 NMR tubes were used for all samples. Previously dialyzed samples were passed through beds of Chelex-100, H^+ form (Bio-Rad), resin held in Pasteur pipets, lyophilized twice from D_2O, dissolved to a concentration of 15 mg/0.5 mL in 100 mM deuterated phosphate buffer (pH 7.4) and degassed by bubbling a stream of argon through the solution while sonicating. Spectra were referenced to an external standard of TSP [3-(trimethylsilyl)propionic-*2,2,3,3-d*$_4$ acid, sodium salt; δ 0 ppm ^{13}C and ^{1}H]. One-dimensional ^{13}C {^{1}H} spectra were acquired at a spectral width of 31 250 Hz (248.6 ppm) with Waltz-16 composite pulse proton decoupling (Shaka et al., 1983) and a 45° observe pulse or by using inverse-gated proton decoupling (10 s interscan delay) to remove

the NOE for signal integration. To optimize line shape, native alginate solutions were acquired at 363 K and fragment spectra at 315 K. ^{1}H spectra were acquired with presaturation of the residual HOD signal on nonspinning samples. Two-dimensional ^{13}C−^{13}C COSY (Bodenhausen et al., 1984) and DQF-COSY (Piantini et al., 1982) spectra were acquired with the conventional time-proportional phase incrementation (TPPI) (Bodenhausen & Ruben, 1980) DQF-COSY pulse sequences, with carbon parameters and composite pulse proton decoupling. A recycle delay of 2 s was used throughout. Spectral widths in both F_1 and F_2 were 31 250 Hz, with a data size of 1K in F_2. A total of 512 t_1 experiments were acquired, and F_1 was zero-filled to 1K. An 60°-shifted sine-bell squared apodization window was applied in both dimensions, and no baseline correction was employed. Inverse double- and triple-quantum spectra were acquired on nonspinning samples in the phase-sensitive mode using TPPI and a pulse program modified from that of Pratum (Pratum & Moore, 1993). These experiments used a 2512 Hz spectral width for ^{1}H in F_2 and a 25 000 Hz spectral width for ^{13}C in F_1. The ^{13}C transmitter was placed at 98.0 ppm. The data size in F_2 was 1K, and 256 experiments were taken with F_1 zero filled to 512 words. Apodization was as given above. T_1 measurements were made with the standard D1−$(180)_x$−τ−$(90)_x$−ACQ pulse sequence, where τ is the variable delay and D1 is a 30 s recovery delay. Raw NMR data was processed and analyzed using the Felix 2.3 package (Biosym Technologies) on a Silicon Graphics Indigo XS 24 workstation. Gaussian line deconvolution for precise satellite integration was accomplished with a line-fitting routine risident in the Felix 2.3 package (Biosym Technologies). ^{1}H- and ^{13}C-NMR assignments are based on the literature reports of our laboratory (Steginsky & Beale, 1992) and of others, as well as on fundamental chemical shift theory.

RESULTS

NMR Spectroscopy of Native Alginate Samples. NMR spectroscopy is the primary tool in the characterization and analysis of bacterial alginate, as well as in the investigation of its biosynthesis. As such, a brief discussion of the special problems presented to the investigator by carbohydrate polymers in NMR experiments is cogent. NMR spectra of native bacterial alginates must be interpreted as representing complex, multicomponent systems instead of a single, unique species. Alginates are polydisperse like most biological polysaccharides, and a single sample may contain a range of chain lengths. Dialysis was used to enrich the high molecular weight fraction (above 3500) to limit the range of rotational correlation times and nuclear relaxation rates for the samples. This treatment was necessary to ensure that inverse-gated decoupling would remove the nuclear Overhauser effect uniformly. When carbon line widths were assessed by peak fitting, it was found that the poly-ManA and poly-GulA fractions possessed average line widths of 1.50 Hz. Alginate, prior to hydrolysis, demonstrates line widths of about 6 Hz. The line width of the low molecular weight component (<3500) was not measured. Polydispersity causes no chemical shift complications because the ^{1}H and ^{13}C resonance frequencies for the various homologues are nearly identical. Signal interpretation is, however, complicated by the block domain structure of the alginate. Native bacterial alginates contain block domains of poly-ManA and poly-GulA, regions in which the monomer types alternate randomly, and transitional regions connecting the previous types of structures (Steginsky & Beale, 1992; Larsen & Haug, 1971a,b; Stokke et al., 1991). Each of these structural typs causes a unique resonance signature. ^{1}H- and ^{13}C-NMR spectra contain the distinct resonances of each and must be treated as composites. Chemical shift assignments for ^{1}H and ^{13}C are presented in Table 1, along with the carbon assignments of sequence triads (Grasdalen et al., 1981). The integrals of the NMR signals from each subtype are proportional to their "concentrations" and are quite reliable when used to compute alginate compositions. Fractional composition data used with Markovian statistical methods (Grasdalen & Larsen, 1979) furnish the only reliable approach to describing native alginate. We used the methods of Grasdalen and Larsen to obtain a description of our native alginate by ^{1}H-NMR. The integral of the G-1 peak (δ 5.05 ppm) equaled 3.8, while those of the M-1/GM-5 peak (δ 4.57 ppm) and the GG-5 peak (δ 4.45) equaled 18.2 and 1.0, respectively. Using the Markovian formulas, the mole fractions (F_X) of each monomer and diad type were calculated. The polymer was found to be largely mannuronate, as $F_M = 0.8$. By difference, then $F_G = 0.2$. Hence the M/G ratio was 4.0. The diad frequencies F_{MM}, F_{GM}, and F_{GG} were calculated to be 0.65, 0.14, and 0.052, indicating a high proportion of mannuronic acid. The sequence distribution parameter (η) was 0.9, consistent with a blockwise distribution of M and G throughout the alginate. The composition parameters for native alginate and that from two feeding experiments are presented in Table 2.

The ^{13}C-NMR spectra of alginate and its fragments can be divided into four distinct regions: the carbinol methine region with resonances from δ 60 to δ 85 ppm; the anomeric region resonating from δ 95 to δ 110 ppm, the carbonyl region at δ 170−180 ppm, and the acetyl methyl region at about δ 35 ppm. The latter region is occupied only in native alginate, since acetyl groups are cleaved during acid hydrolysis of the polymer. Natural abundance spectra were acquired for all samples as a baseline, and Table 1 shows the chemical shift data. In the broad-band decoupled spectra of the oligosaccharide fragments, a weak signal for the reducing end anomeric carbon is visible at δ 95 ppm. In ^{13}C-NMR spectra, the signals of the center residue of each possible "triad" (e.g., MMM, GGG, MGM, GMG) resonate at unique frequencies. The extremes are, of course, pure poly-ManA (MMM) and poly-GulA (GGG), and these triads will dominate if the alginate is enriched in block structure.

Table 1: Proton Chemical Shift Assignments for Polyguluronate and Polymannuronate[a]

proton	L-guluronan	D-mannuronan
H-1	5.03, d, $J_{1,2} = 4.4$	4.57, s
H-2	3.89, dd, $J_{1,2} = 4.4$, $J_{2,3} = 3.7$	3.95, d, $J_{1,2} = 0$, $J_{2,3} = 3.3$
H-3	3.99, dd, $J_{2,3} = 3.7$, $J_{3,4} = 4.2$	3.66, dd, $J_{2,3} = 3.3$, $J_{3,4} = 9.2$
H-4	4.10, dd, $J_{3,4} = 4.2$, $J_{4,5} = 0$	3.81, dd, $J_{3,4} = 9.2$, $J_{4,5} = 9.6$
H-5	4.44, s	3.65, d, $J_{4,5} = 9.6$

[a] d = doublet; dd = doublet of doublets; s = singlet.

Table 2: Statistical Characterization of Three Types of Alginate by the Markovian Method[a]

alginate	I_A	I_B	I_C	F_M	F_G	F_{MM}	F_{MG}	F_{GM}	F_{GG}	η	M/G
native	1.0	4.78	0.26	0.80	0.20	0.65	0.15	0.15	0.05	0.92	4.00
[U-^{13}C$_6$]Alg	1.0	1.23	0.81	0.51	0.49	0.42	0.10	0.10	0.40	0.38	1.04
[1-^{13}C]Alg	1.0	2.31	00.47	0.64	0.36	0.45	0.19	0.19	0.17	0.83	1.77

[a] For $\eta < 1$ the chains possess block domain structures. For η approximately equal to 1 the structure is random.

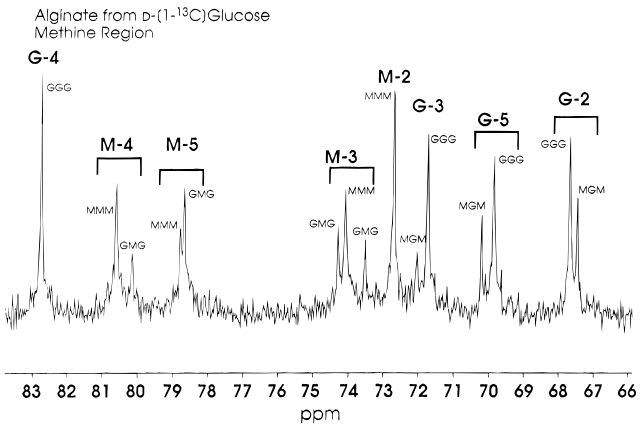

FIGURE 3: Upfield expansion of the ^{13}C-NMR spectrum of alginate. Resonance regions for carbon atoms are marked, and triads are highlighted.

The center triad resonance may be integrated and used in a triad frequency calculation to get a statistical description of the polymer. Figure 3 shows the upfield region of a ^{13}C-NMR spectrum of native alginate, with the triad assignments indicated. A confirmatory check on the proton data was made with ^{13}C-NMR spectroscopy, and assignments were verified for our isotope studies. Our ^{13}C-NMR data for native alginate supported the conclusions drawn from the proton studies.

^{1}H- and ^{13}C-NMR experiments were also used to characterize the fractional oligo-ManA and oligo-GulA obtained by depolymerization of alginate. These samples showed no evidence of contamination by other sugar sequences. The ratio of the integral of $H1_{reducing}$ to $H1_{internal}$ indicated that the oligomers were of an average degree of polymerization (dP) of ≈20, consistent with our dialysis cutoff. At this chain length, ^{13}C inversion−recovery T_1 measurements at 125 MHz yielded relaxation times of 480 ms for internal ring carbons and 4.5 s for the carboxylates. Upon resolution enhancement, the ^{1}H−^{1}H coupling constants could be measured for ring protons and were completely consistent with our previous work and that of others.

Feeding Experiments with D-*[1-^{13}C]Glucose*. A preliminary experiment was conducted with D-[1-^{13}C]glucose to estimate the amount of precursor catabolism. The results of this experiment helped us to fine-tune our experimental protocol and provided information on the extent of isotope scrambling during biosynthesis. *A. vinelandii* NCIB-8789 was cultivated in a medium containing glucose at an initial isotope dilution of 12.5 atom % ^{13}C; glucose ^{12}C and the alginate were isolated and purified by our usual procedure. There were a number of noteworthy features in this spectrum: (1) The inverse-gated decoupled ^{13}C{^{1}H} spectrum of the native alginate showed approximately a 15% enhancement in integrated signal for all anomeric carbons (C1) at approximately δ 101 ppm, as compared with an identically prepared and acquired native sample. The integral is also internally consistent with other nonenriched carbon atom signals. (2) The *relative* intensities of the anomeric signals were unchanged. (3) The integrals of all other signals remained at natural abundance within experimental error. (4) In spectra of [1-^{13}C]glucose-labeled poly-ManA and poly-GulA the relative changes in integrated signal were the same as those for the alginate itself. The inverse-gated decoupled spectrum is shown in Figure 4, and Figure 5 shows an integrated upfield expansion of high-mannuronate native

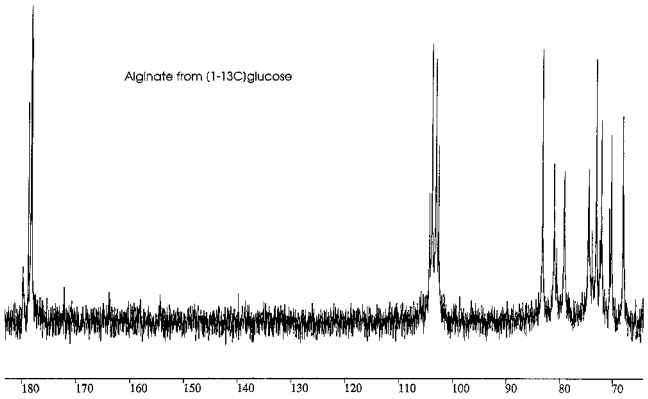

FIGURE 4: Inverse-gated decoupled ^{13}C-NMR spectrum of alginate from a [1-^{13}C]glucose feeding.

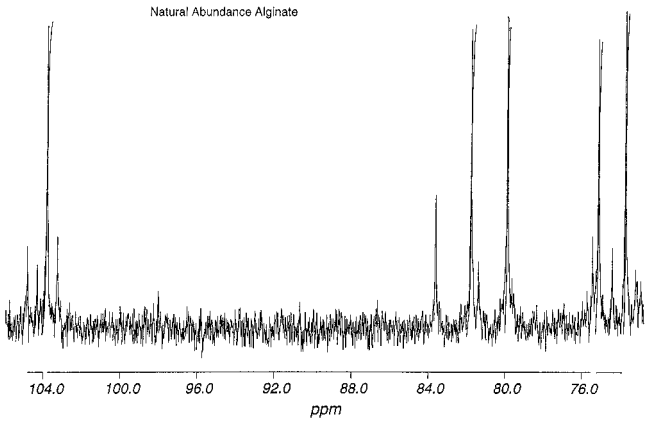

FIGURE 5: Integrated inverse-gated decoupled ^{13}C-NMR spectrum of nonlabeled alginate showing the equalization of line intensities upon removal of the nuclear Overhauser effect.

alginate. The efficiency of the inverse-gated decoupling is evident from the nearly identical integrals of the ManA signals. These observations suggested that this substrate, while being partly catabolized prior to alginate biosynthesis, provided substantial enrichment in the product with little or no scrambling of isotope from C1 to other carbon atoms. The data supported the notion that successful labeling from multiply-labeled glucose would be possible. The data from the [1-^{13}C]glucose feeding are also consistent with some "direct" incorporation of label from the precursor through fructose. Most notably, label did not detectably partition from C1 of the precursor into C6 of the product. This tends to rule out the Embden−Meyerhof−Parnas pathway as the primary pathway of substrate catabolism. Ring inversion of glucose by reduction at C1 to D-sorbitol 6-phosphate (the same compound as L-gulitol 1-phosphate), followed by oxidation of L-gulitol 1-phosphate to guluronic acid and activation as a GDP sugar, is also unequivocally ruled out. This pathway, a long-debated potential route of guluronate formation (Russel & Gacesa, 1988), would require that label from C1 of the precursor be transferred into C6 of the product. Clearly this is not the case.

Feeding Experiments with [2-^{13}C]Glucose. Glucose labeled at the 2-position is a sensitive tool for assessing catabolism by the phosphogluconate (pentose phosphate) pathway (Sanders & Jones, 1989). One can show on paper that the transketolase and transaldolase reactions of the pentose phosphate shunt partition label from glucose specifically into C1 and C3 of product hexoses; any label in the C2 position must result from either direct incorporation or catabolism of the precursor through the Entner−Doudoroff

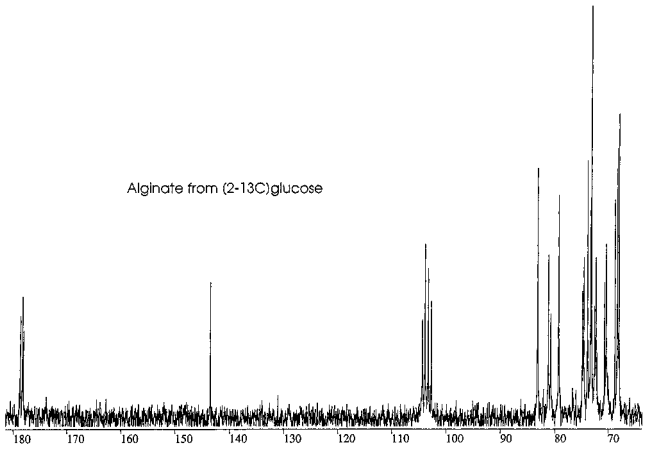

FIGURE 6: Inverse-gated decoupled ^{13}C-NMR spectrum of alginate from a [2-^{13}C]glucose feeding.

or Embden−Meyerhof−Parnas pathways. Additionally, entry into this pathway involves the obligatory loss of C1 as CO_2 to form ribulose 5-phosphate. Features of the spectrum of alginate resulting from this feeding experiment were as follows: (1) The inverse-gated $^{13}\{^1H\}$ spectrum of native alginate labeled from [2-^{13}C]glucose showed that the integral of the C2 carbon region (68−72 ppm) was increased by a factor of 2.1 in both the ManA and GulA blocks. (2) The integrals of the C1 and C3 carbon regions (100, 74 ppm) had each increased by a factor of 1.2. These enhancements were determined by comparison with an identical sample and by internal comparison as well. The spectrum is presented in Figure 6. These results are consistent with catabolism through either the E−M−P or E−D pathways, as well as with direct incorporation of the hexose skeleton via fructose. Additionally, a small amount of the precursor appears to be cycling through the pentose phosphate pathway from glucose to fructose, causing redistribution of label into C1 and C3. In the spectrum shown in Figure 6, the sharp resonance at approximately 145 ppm is present only in this sample. Its origin was traced to a contaminant in the sample buffer.

Feeding Experiments with [6-^{13}C]Glucose. A sample of alginate from D-[6-^{13}C]glucose was obtained and analyzed by $^{13}C\{^1H\}$ NMR. We also obtained a pure sample of poly-ManA from a hydrolysis, and the ^{13}C-NMR spectrum of the oligomeric material revealed only two equally enhanced signals; the C6 signal at δ 178.0 ppm and the C1 signal at δ 102.8 ppm. The intensities of lines from these positions were approximately doubled as compared to signals from any other position in the molecule and were much greater than those for samples from either of the other singly labeled glucose feedings. The noise level precluded signal integration for accurate quantitation, but relative intensity comparisons based upon the inverse-gated decoupled ^{13}C-NMR spectrum of unlabeled poly-ManA clearly show the enrichments. The spectrum of the native poly-ManA showed equalized line intensities, indicating that the nuclear Overhauser effect had been eliminated. The same experiment performed at different times on different poly-ManA samples was completely reproducible. The spectrum of poly-ManA labeled from [6-^{13}C]glucose is shown in Figure 7a. The sample of native alginate as an equivalent sample showed the same equal C1 and C6 enrichments, and the labeling was, as expected, identical in the block, random, and transitional regions. This spectrum is shown in Figure 7b. The equally high incorporation rates at C1 and C6, in contrast with the

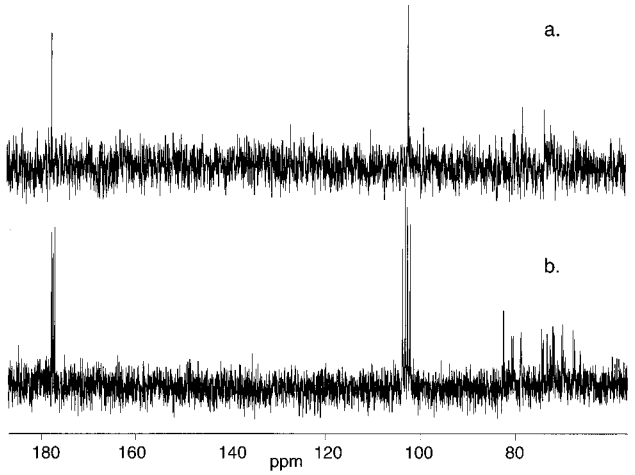

FIGURE 7: (a) Inverse-gated decoupled ^{13}C-NMR spectrum of poly-ManA from a [6-^{13}C]glucose feeding. Only C1 and C6 are enriched. (b) Corresponding inverse gated-decoupled ^{13}C-NMR spectrum of alginate from a [6-^{13}C]glucose feeding.

Table 3: Carbon-13 NMR Assignments of Alginate Monomers[a]

	resonance position of center carbon					
triad	C1	C2	C3	C4	C5	C6
MMM	102.7	72.3	73.7	80.3	76.8	175.7
MMG	103.9	73.3		82.3	79.1	177.5
GMM	102.7	72.7		81.2	79.7	177.4
GMG	103.8	73.3	74.3	81.2	78.8	178.5
GGG	103.3	67.5	71.5	82.6	69.5	177.8
GGM	102.3	68.8		82.6	71.3	177.4
MGG	103.4	69.2		82.6	71.1	177.3
MGM	101.9	69.3	72.1	82.6	71.3	178.4

[a] The chemical shift position of the center carbon atom of each triad type is given.

single partitioning of C1 label from precursor into C1 of the product residues, are consistent with the notion of the Entner−Doudoroff pathway as the primary route of catabolism.

Feeding Experiments with [U-$^{13}C_6$]Glucose. A biosynthetic sample of native alginate was prepared by growing *A. vinelandii* on a medium with an overall enrichment of 12.5% w/w [U-$^{13}C_6$]glucose:nonlabeled glucose. The resulting one-dimensional $^{13}C\{^1H\}$ spectrum showed extensive homonuclear coupling as evidenced by numerous ^{13}C satellites flanking noncoupled signals. The spectrum of native alginate is complicated by signal overlap, but contributions from at least five of the eight possible triad types could be seen in the less cluttered C1 and C6 regions of resolution-enhanced spectra of high digital resolution (Table 3). For discussion purposes, Figure 8 shows a spectrum of poly-GulA, which is less cluttered. The signals from mannuronate carbon atoms are more intense than those of guluronate. This indicates in part that, as expected from our production conditions, the ManA content of the polymer is higher than that of GulA. Satellite signals at C1 and C6 of both monomer types are clearly doublets ($^1J_{CC}$ = ca. 45 and 59 Hz, respectively), while the C2 and C5 regions of both appeared to contain doublet of doublets ($^1J_{CC}$ = ca. 45 Hz), consistent with AMX patterns. These data suggested that ManA and GulA residues both contained two doubly coupled systems from incorporation of 3-carbon units. Interestingly, a first-order analysis of the intensities of the satellite signals indicated that the absolute enrichments in the ManA units were greater than the corresponding ones in GulA. From the 1D spectrum of

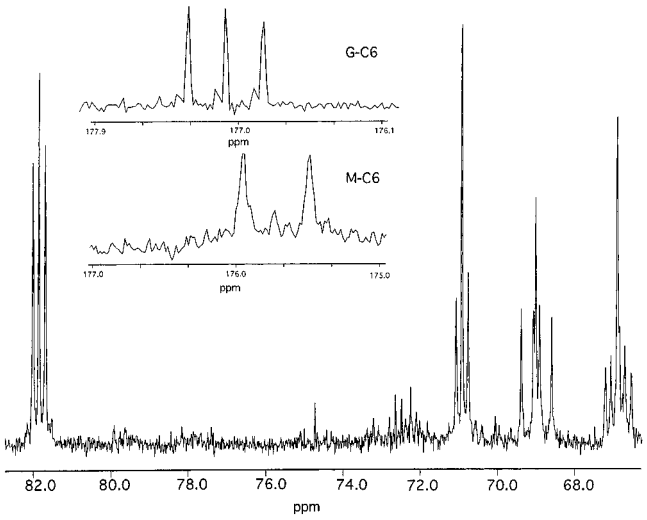

FIGURE 8: Expansion of the ^{13}C-NMR spectrum of poly-GulA from the [U-$^{13}C_6$]glucose feeding. The inset compares the anomeric resonances of poly-ManA and poly-GulA, showing the higher enrichment in the former.

native alginate it was not possible to resolve the two-bond carbon−carbon couplings of the AMX systems.

In order to completely measure the AMX patterns, since one-dimensional ^{13}C-NMR spectra of native alginates were complicated by signal overlap and broad lines, the sample was hydrolyzed and purified blocks of poly-ManA and poly-GulA of dP $\approx$ 20 were prepared. Spectra of these samples each displayed six signals representing degenerate contributions of carbon atoms of the uronate residues. A small signal could be identified for the reducing end anomeric carbon atom. Figure 8 presents the spectrum for oligo-GulA. The inset shows the anomeric region with the ManA signal superimposed. The higher enrichment in ManA is indicated by the more intense satellites. These spectra were simplified enough that most of the ^{13}C coupling patterns could be discerned, but smaller two-bond couplings were still unobservable. Absolute enrichment (as given by percent coupling to neighboring atoms) was determined by integration of satellites after Gaussian deconvolution of the lines. The sample of poly-GulA appeared to possess two AMX-type spin systems, as evidenced by the four-line patterns of signals of C2 (δ 67.8) and C5 (δ 69.9), each the center carbon atom of an AMX-type spin system. No evidence of two-bond coupling was observed at C1, C3, C4, or C6. The satellite signals for C5 at δ 69.9 formed a clear doublet of doublets ($J_{4,5}$ = 40 Hz, $J_{5,6}$ = 59 Hz). The satellite pattern at C-2 was more complex. In this case, $J_{1,2}$ and $J_{2,3}$ were almost identical at 45 Hz, and the inner lines overlap to form a pseudotriplet coincident with the noncoupled line. Upon resolution enhancement these lines could be measured. Additionally, two satellite lines lie midway between the center and outer lines. These were determined to represent a singly coupled system with $^1J_{CC}$ = 45 Hz. This finding provided evidence of a second isotopomer, containing a singly coupled, two-carbon system at C1/C2, superimposed on a doubly coupled C1/C2/C3 system. The singly coupled system is consistent with a prominent isotopomer from the pentose phosphate shunt (Jones & Sanders, 1989). The average enrichment in the GulA residues was found to be 35%.

Analysis of the poly-ManA sample led us to propose the same coupling pattern, differing from the GulA pattern only in the absolute enrichment. In this case, the average enrichment as percentage of coupled signal was about 85%, significantly higher than that for the GulA blocks. A phase-sensitive TPPI double-quantum-filtered COSY experiment encompassing the spectral region from 180 to 50 ppm allowed us to confirm the assignments of all of the carbon atoms and facilitated the identification of the coupling networks in the alginate molecule. As has been shown, ^{13}C−^{13}C DQF-COSY provides an excellent alternative to ^{13}C homonuclear decoupling and 2D INADEQUATE (Bax et al., 1981) techniques for tracing biochemical connectivities, as has been shown and quantified (Jones & Sanders, 1989). The simplified diagonal permits analysis of even poorly dispersed signals, and the characteristic cross-peak phase patterns allow signals containing more than one coupling contribution to be identified and quantitated. In our experiments, the biochemical connectivity could be traced for native alginate as well as for poly-ManA and poly-GulA and suggested that the molecules contained two AMX-type systems, indicating intact incorporation of two three-carbon units per hexose. The most important information from the DQF-COSY experiments was, however, the accurate values of the satellite coupling constants in crowded spectral regions.

Table 4: Predicted and Observed ^{13}C/^{1}H Inverse Double-Quantum Responses of Alginate Labeled from [U-^{13}C]Glucose[a,b]

carbon atoms		∂ (in Hz) from transmitter		double-quantum frequency (Hz)	
				predicted	
A	B	A	B	A + B	obsd
G1	G2	+666.2	−3796.1	−3129.9	−3131.1
G2	G3	−3796.1	−3293.3	−7089.4	−7098.1
G3	G4	−3293.3	−1935.7	−5229.1	not obsd
G4	G5	−1935.7	−3532.2	−5467.8	−5465.0
G5	G6	−3532.2	+9678.2	+6145.6	+6460.1
M1	M2	+603.3	−3243.0	−2639.0	−2637.5
M2	M3	−3243.0	−2966.5	−6209.5	−6212.1
M3	M4	−2966.5	−2174.6	−5141.1	not obsd
M4	M5	−2174.6	−2400.8	−4575.4	−4570.2
M5	M6	−2400.8	+9930.0	+7530.3	+7790.1

[a] Double-quantum responses are recorded as the algebraic sums of the ^{13}C chemical shifts relative to the transmitter. [b] Carbon transmitter positioned at 98.0 ppm.

DQF-COSY data provide no information on intact incorporation of label in more than two adjacent carbon atoms. In other words, if there is an intact three-carbon unit at atoms A−B−C, the DQF-COSY would allow the A−B and B−C couplings to be identified but would not allow combinations of these two isotopomers to be distinguished from the three-atom combination. We developed the triple-quantum INADEQUATE experiment (Beale et al., 1987; Braunschweiler et al., 1983) to specifically select intact three-carbon systems. This ^{13}C-detected experiment, however, is much too insensitive for application to the alginates. Combining generation of carbon triple-quantum coherence, or simultaneous three-spin flips, with an inverse INEPT detection sequence allows the evolution of ^{13}C triple-quantum (TQ) frequencies to be mapped into ^{1}H observation. Obviously, due to the difference in the magnetogyric ratios of carbon and proton, and the polarization transfer of the INEPT sequence, a substantial gain in sensitivity is obtained. We ran inverse double-quantum (DQ) and TQ experiments (Pratum & Moore, 1993) on samples of poly-GulA and poly-ManA. Tables 4 and 5 show the data from these experiments. Clearly, while the DQ experiment, exciting and detecting simultaneous double

Table 5: Predicted and Observed Triple Quantum Responses of Alginate Labeled from [U-^{13}C]Glucose[a,b]

carbon atoms			∂ (in Hz) from transmitter			triple-quantum frequency (Hz)	
						predicted	
A	B	C	A	B	C	A + B + C	obsd
G1	G2	G3	+666.2	−3796.1	−3293.3	−6423.2	−6430.0
G4	G5	G6	−1935.7	−3532.2	+9678.2	+4210.3	+4220.1

[a] Triple-quantum responses are recorded as the algebraic sums of the ^{13}C chemical shifts relative to the transmitter. [b] Carbon transmitter positioned at 98.0 ppm.

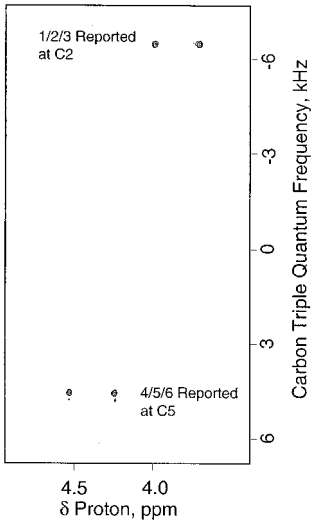

FIGURE 9: Plot of the inverse triple-quantum spectrum of poly-GulA.

spin flips, provides information on singly coupled (two-carbon) systems, it will not selectively reveal three-carbon, doubly coupled AMX systems. The TQ spectrum of poly-GulA, shown in Figure 9, unequivocally reveals the presence of two doubly coupled units. The TQ frequencies −6423.2 Hz for G1/G2/G3 and +4210.3 for G4/G5/G6, are reported at the proton frequency of the center methine proton of the three-carbon unit. The predicted TQ frequencies, given as the algebraic sums of the chemical shifts relative to the carbon transmitter, are in excellent agreement with the experimental values. The TQ spectra therefore confirm the presence of two doubly coupled units of equal abundance in each hexose unit.

DISCUSSION

The principle of biosynthetic experiments with multiply ^{13}C-labeled precursors relies upon two factors: scalar coupling between spin $-^1/_2$ nuclei and metabolic dilution. If a precursor is fed that is enriched with ^{13}C in two adjacent carbon atoms in the *same molecule*, for example, [1,2-$^{13}C_2$]-acetate, incorporation of the precursor without cleavage of the labeled bond is demonstrated by coupling of each signal to give a doublet (Floss & Beale, 1989). The typical appearance of data from a situation such as this will be a set of satellite signals flanking a central, noncoupled line. The satellites in a simple two-spin system such as this will form an AB- or AX-type spin system, and each doublet will report the *J*-coupling to its neighbor. For the purposes of this work, such a system will be called "singly coupled". If, during metabolism, the precursor undergoes bond scission between the labeled atoms, metabolic dilution from nonlabeled metabolic pools will make it improbable that both labels will occur together in the same product molecule. Hence, AB or AX coupling will be lost. If the labeled bond is incorporated without scission, the chances that both atoms are incorporated together *in the same molecule* is essentially 100%, and *J*-coupling will be observed, depending upon the absolute enrichments at the labeled atoms. Integrating the satellites reports the amount of coupling of a given carbon atom to its neighbor, and the amount of scission can be estimated. The situation becomes much more complex for precursors containing three or more coupled nuclei. A three-spin (^{13}C−^{13}C−^{13}C) incorporation will yield a 12-line AMX pattern in the product and will be referred to as "doubly coupled".

The precursor D-[U-$^{13}C_6$]glucose is a powerful tool for the assessment of metabolism. The extremely complex coupling patterns present in the precursor itself are simplified by catabolism through any number of pathways, giving rise to readily interpretable patterns. If, for example, the Embden−Meyerhof−Parnas pathway were the sole route of catabolism of glucose, metabolism into an equilibrated triose pool and resynthesis of hexoses will give rise to two doubly coupled AMX satellite systems of equal intensity in the product. Catabolism through the pentose phosphate pathway can produce eight unique isotopomers, containing superimpositions of singly and doubly coupled systems. The challenge in interpretation is to filter the multiply coupled patterns from each other and from overlapping noncoupled lines. Most often, spectral overlap, weak satellites, and superimpositions of patterns from multiple pathways render a first-order analysis impossible. A number of two-dimensional NMR techniques have been applied to problems such as these, including double- and triple-quantum INADEQUATE, ^{13}C homonuclear *J*-spectroscopy, and phase-sensitive ^{13}C homonuclear DQF-COSY. The double-quantum experiments filter singly coupled systems from the background but will not allow separation of doubly coupled units. This is the function of the triple-quantum experiment. Properly acquired, a TQ spectrum will contain signals only from doubly coupled systems, allowing their unequivocal identification (Braunschweiler et al., 1983). Newer variations include inverse (proton-detected) multiple-quantum spectroscopy. Typically, combinations of these techniques are used.

The results of our experiments with singly labeled glucoses were, in general, consistent with earlier radioisotope studies. Carlson and Matthews (1966) studied mucoid strains of *P. aeruginosa* and demonstrated that radiolabel from [6-^{14}C]-glucose was incorporated into an acidic polysaccharide fraction from culture broth 160 times more efficiently than was [1-^{14}C]glucose. These studies, which measured radioactivity from C6 in CO_2 captured after decarboxylating the sugar, demonstrated that glucose was incorporated into the polymer without randomization or inversion of the carbon skeleton. No unequivocal determination of the identities of the polymers as alginate, polymannuronate, or polyguluronate was made in this work. A seminal study of alginate biosynthesis in *A. vinelandii* was reported by Pindar and Bucke (1975). This work demonstrated for the first time that polymannuronic acid is the first polymeric substance formed in alginate biosynthesis and that mannuronate is apparently epimerized at the polymer level to form the guluronic acid units of alginate. Lynn and Sokatch reinvestigated 1-, 2-, and 6-[^{14}C]glucose incorporation in parallel studies on *P. aeruginosa* and *A. vinelandii* (Lynn & Sokatch, 1984). They found a 10-fold greater incorporation rate of

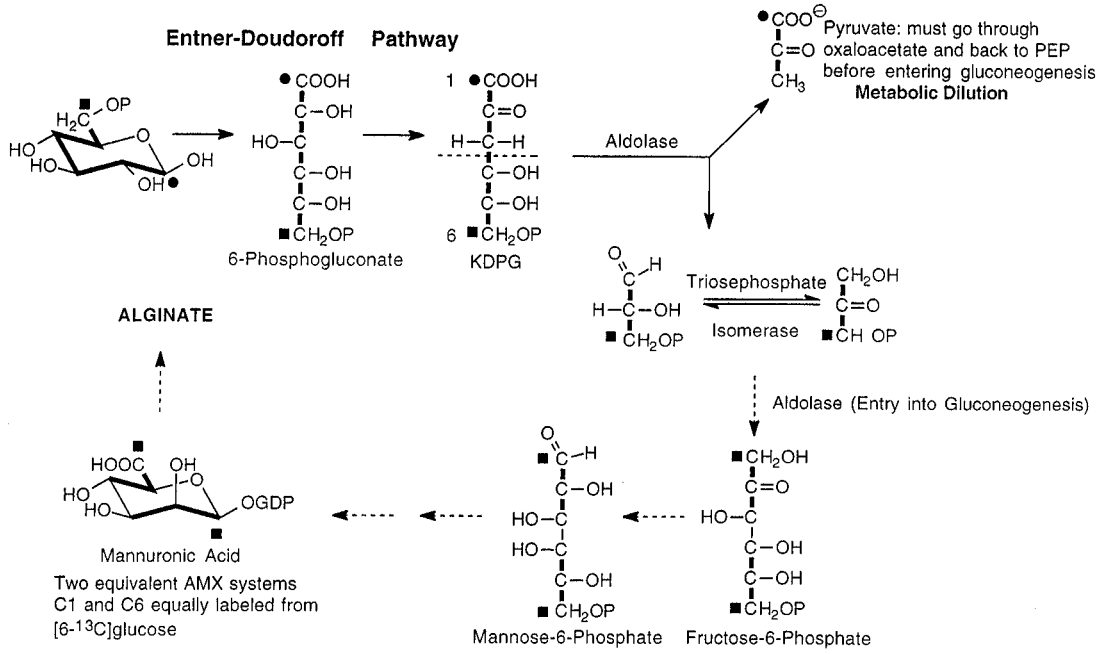

FIGURE 10: Depiction of the carbohydrate flux through the E−D pathway and into alginate biosynthesis.

label from [6-^{14}C]glucose than for [1-^{14}C]glucose. Though their specific incorporation rates were lower, the results generally agree with Carlson's work. The experiments of Wingender et al. (1985) yielded essentially the same information. In the latter two studies, no degradation of the sugars was performed to rule out scrambling of the label or the presence of competing metabolic pathways. Anderson et al. (1987) measured the incorporation of label from glucose and fructose in parallel experiments. Both *Pseudomonas mendocina* and *A. vinelandii* incorporate radiolabel from fructose equally well from the 1- and the 6-positions, whereas labeled glucose provided the typical higher incorporation rate from C6 than from C1. All of these findings suggest that there is an obligatory intermediacy of three-carbon (triose) intermediates as precursors to alginate when the organism is growing on glucose. These findings are all consistent with the Entner−Doudoroff (E−D) pathway as the primary catabolic pathway for glucose and the feedstock for hexose precursors of alginate in these organisms. Our own work greatly clarifies and expands these ideas. The incorporation of [1-^{13}C]- and [2-^{13}C]glucose into alginate was in accord with a minor amount of "direct" incorporation through fructose 6-phosphate. A small amount of partitioning of label from C2 of glucose into C1 and C3 of the product was observed, indicating that the pentose phosphate pathway may be contributing to the overall labeling pattern. This notion is supported by the finding of a C1/C2-coupled unit in ManA and GulA regions and by the observation of Sokatch, who found that label from C2 is incorporated into alginate at a rate twice as high as that at C1. The lack of evidence for significant loss of C1 of glucose as $^{13}CO_2$ means that the pentose phosphate pathway is probably minor in this biosynthetic scheme. The incorporation rates of the C1- and C2-labeled precursors were low and were only measurable with inverse-gated ^{13}C-NMR spectroscopy. Nevertheless, the key findings from these two sets of experiments are as follows: (1) There is no apparent transfer of label from C1 of the precursor into C6 of the product. This fact tends to exclude the Embden−Meyerhof−Parnas pathway from consideration since label from these positions equilibrates at the triosephosphate isomerase step. (2) Since label from C1 of the precursor did not transfer into C6 of the product, the possibility of guluronate synthesis by skeletal inversion (oxidation of glucose to gluconic acid, then reduction to L-guluronate) may be eliminated.

Unequivocal proof of the biosynthetic flux was obtained with a feeding experiment of [U-$^{13}C_6$]glucose. The 99 atom % labeled glucose, if incorporated directly through fructose, would cause an extremely complex six-spin coupling pattern, with all signals multiply coupled. No evidence of completely coupled hexose was found in the alginate or the oligomers. Instead, the first-order ^{13}C-NMR analysis showed much simplified systems resembling AMX patterns for two doubly coupled spin systems per hexose. The lack of a resolved J_{AX} for the AMX systems, and the closeness of the J_{AM} and J_{MX}, made direct first-order spin system identification equivocal.

The two-dimensional double-quantum ^{13}C-COSY (DQF-COSY) has been used for biosynthetic analysis for years. In our hands, the COSY experiment allowed us to trace the C1−C2, C2−C3, C4−C5, and C5−C6 connectivities, but the DQ experiment is not capable of identifying doubly coupled systems and separating them from singly coupled ones. A doubly coupled system looks just like two singly coupled ones in this experiment. Since the J_{AX} coupling was not resolved, the active/passive splitting approach of Jones and Sanders (1989) was not possible.

The inverse triple-quantum (TQ) experiment provided the solution to the problem of identifying doubly coupled spin systems in the molecules. The TQ experiment showed two clean sets of cross-peaks representing C1/C2/C3 and C4/C5/C6, each reported at the center carbon of the triad. A critical feature of this experiment is that though J_{AX} is not resolved, the TQ response is still reported at the frequency of M. The TQ experiment establishes that there are two doubly coupled spin systems per hexose unit, indicating that two intact trioses were incorporated. Notably, the cross-peaks for the C1/C2/C3 system and the C4/C5/C6 system are of equal intensity.

The feeding experiment with [6-^{13}C]glucose provided confirmation of the [U-^{13}C]glucose results in native alginate

and the oligomers. Label from this precursor partitioned equally and efficiently into C1 and C6 of the product. In the alginate, the signals had increased by a factor of 2, whereas in the poly-ManA they were 8-fold more intense than natural abundance. This difference may be attributed to the faster relaxation rate and narrower lines of the poly-ManA.

Taken together, our results provide a complete picture of the metabolic flux from glucose to alginate in *A. vinelandii*. The proposed model is shown in Figure 10. If the Embden−Meyerhof pathway were the main route of catabolism, we would expect label from C1 and C6 of the precursors to equilibrate, and unless the triose pools are not in equilibrium, the C1/C2/C3 portions of each ring should be enriched identically to C4/C5/C6. Clearly, C1 did not transfer into C6, and the incorporation rate from the 1-labeled glucose was low, implying that extensive dilution was occurring. The triose pools at the base of the Embden−Meyerhof pathway branch into anapleurotic reactions, and dilution is high. The Entner−Doudoroff pathway utilizes a bifurcated route. Here, the aldolase reaction forms pyruvate and glyceraldehyde 3-phosphate. In order to be passed into gluconeogenesis, the pyruvate (from C1/C2/C3 of the precursor) must be converted to oxaloacetate by pyruvate carboxylase and then back to phosphoenolpyruvate by PEP carboxykinase. The glyceraldehyde 3-phosphate representing C4/C5/C6 of the precursor can immediately reenter gluconeogenesis. Both halves of the resynthesized hexose will contain doubly coupled spin systems, and the relative incorporation should be equal. This was in fact what we observed. The circuitous route taken by the pyruvate explains the extensive dilution of label from C1 and makes the contrast with label from C6 more remarkable.

An intriguing finding of this work was the lower enrichment in poly-GulA than poly-ManA fractions. Since we know that poly-ManA is the immediate precursor to alginate, we can postulate that the poly-ManA chain will be more highly enriched on its "starter" end and will demonstrate decreasing enrichment as polymerization proceeds along with metabolic dilution. Since mannuronan C5-epimerase catalyzes formation of GulA units, the fact that they are lower in enrichment than ManA, we may speculate that epimerization begins in more terminal, diluted parts of the chain or proceeds in the same direction as polymerization. In a ^{13}C-NMR spectrum of poly-ManA labeled from [U-$^{13}C_6$]-glucose, it was possible to observe the separate signals for the reducing end of the chain (ca. 95 ppm) and the nonreducing end of the chain (ca. 71 ppm). The nonreducing carbon signal showed nearly 85% coupling, whereas the reducing end signal only was 40% coupled. This indicates that dilution is more pronounced at the reducing end and that polymerization (and epimerization) takes place from the nonreducing end. These data suggest that something analogous to the polyketide "starter unit effect" is occurring in the polysaccharide. While this is not unequivocal proof, these data provide the first information on the directionality of the two terminal biosynthetic enzymes.

ACKNOWLEDGMENT

The authors are grateful for the assistance of Steve Sorey of the Department of Chemistry NMR center and to Dr. Blain M. Mamiya for fruitful discussions.

REFERENCES

Anderson, A. J., Hacking, A. J., & Dawes, E. A. (1987) *J. Gen. Microbiol. 133*, 1045−1052.

Bax, A., Freeman, R., & Frenkiel, T. A. (1981) *J. Am. Chem. Soc. 103*, 2102−2104.

Beale, J. M., Cottrell, C. E., Keller, P. J., & Floss, H. G. (1987) *J. Magn. Reson. 72*, 574−578.

Bodenhausen, G., & Ruben, D. J. (1980) *Chem. Phys. Lett. 69*, 185−188.

Bodenhausen, G., Kogler, H., & Ernst, R. R. (1984) *J. Magn. Reson. 58*, 370−388.

Braunschweiler, L., Bodenhausen, G., & Ernst, R. R. (1983) *Mol. Phys. 48*, 535−540.

Carlsson, D. M., & Matthews, L. W. (1966) *Biochemistry 5*, 2817−2822.

Darzins, A., & Chakrabarty, A. M. (1984) *J. Bacteriol. 159*, 9−18.

Degwert, U., v. Hülst, R., Pape, H., Herrold, R. E., Beale, J. M., Keller, P. J., Lee, J. P., & Floss, H. G. (1987) *J. Antibiot. 40*, 855−861.

Floss, H. G., & Beale, J. M. (1989) *Angew. Chem., Int. Ed. Engl. 28*, 146−177.

Gacesa, P. (1988) *Carbohydr. Polym. 8*, 161−182.

Grasdalen, H., Larsen, B., & Smidsrød, O. (1979) *Carbohydr. Res. 68*, 23−31.

Grasdalen, H., Larsen, B., & Smidsrød, O. (1981) *Carbohydr. Res. 89*, 179−191.

Jones, D. N. M., & Sanders, J. K. M. (1989) *J. Am. Chem. Soc. 111*, 5132−5137.

Knutson, C. A., & Jeanes, A. (1968) *Anal. Biochem. 24*, 482−490.

Larsen, B., & Haug, A. (1971a) *Carbohydr. Res. 17*, 297−308.

Larsen, B., & Haug, A. (1971b) *Carbohydr. Res. 17*, 287−296.

Lin, T.-Y., & Hassid, W. Z. (1966a) *J. Biol. Chem. 241*, 5284−5297.

Lin, T.-Y., & Hassid, W. Z. (1966b) *J. Biol. Chem. 241*, 3283−3293.

Lynn, A. R., & Sokatch, J. R. (1984) *J. Bacteriol. 158*, 1161−1162.

Ohman, D. E., Goldberg, J. B., & Flynn, J. L. (1990) *Molecular Analysis of the Genetic Switch Activating Alginate Production*, pp 28−43, American Society for Microbiology, Washington, DC.

Piantini, U., Sørenson, O. W., & Ernst, R. R. (1982) *J. Am. Chem. Soc. 104*, 6800−6801.

Pindar, D. F., & Bucke, C. (1975) *Biochem. J. 152*, 617−622.

Pratum, T. K., & Moore, B. S. (1993) *J. Magn. Reson. Sect. B 102*, 91−97.

Rohr, J., Beale, J. M., & Floss, H. G. (1989) *J. Antibiot. 42*, 1151−1157.

Russell, N. J., & Gacesa, P. (1988) *Mol. Aspects Med. 10*, 1−91.

Shaka, A. J., Keeler, J., & Freeman, R. (1983) *J. Magn. Reson. 53*, 313−340.

Skjåk-Bræk, G., & Larsen, B. (1982) *Carbohydr. Res. 103*, 137−140.

Steginsky, C. A., Beale, J. M., Floss, H. G., & Mayer, R. M. (1992) *Carbohydr. Res. 225*, 11−26.

Stokke, B. T., Smidsrød, O., Bruheim, P., & Skjåk-Bræk, G. (1991) *Macromolecules 24*, 4637−4645.

Wingender, J., Sherbrock-Cox, V., Gacesa, P., & Russell, N. J. (1985) *Biochem. Soc. Trans. 13*, 1148−1149.

Zielinski, N. A., DeVault, J. D., Roychoudhury, S., May, T. B., Kimbara, K., Kato, J., Shinabarger, D., Kitano, K., Berry, A., Misra, T. K., & Chakrabarty, A. M. (1990) Molecular Genetics of Alginate Biosynthesis in *Pseudomonas aeruginosa*, in *Pseudomonas; Biotransformations, Pathogenesis, and Evolving Biotechnology* (Silver, S., Chakrabarty, A., Iglewski, B., & Kaplan, S., Eds.) pp 15−27, ASM Publications, Washington, DC.

BI951922V